Available online at www.sciencedirect.com
SCIENCE DIRECT®
Journal of the European Ceramic Society 25 (2005) 2655–2659
www.elsevier.com/locate/jeurceramsoc

The effect of reduction atmosphere on the $LaGaO_3$-based solid oxide fuel cell

Jae Yeon Yi, Gyeong Man Choi *

Department of Materials Science and Engineering, Pohang University of Science and Technology, San 31, Hyoja-dong, Pohang 790-784, Republic of Korea

Available online 23 March 2005

Abstract

Chemical stability of $La_{0.9}Sr_{0.1}Ga_{0.8}Mg_{0.2}O_3$ (LSGM) as an electrolyte for solid oxide fuel cells (SOFCs) was investigated. At low oxygen-partial pressure (0.003 atm), the LSGM electrolyte partly decomposed due to the development of high overpotentials, and thus the induced reduction atmosphere near cathode. The morphology of LSGM grain near cathode changed due to the formation of new phases. The main decomposition phases were La_2O_3, $La(OH)_3$ and $LaSrGaO_4$. The polarization conductance increased due to the microstructural change in LSM and thus the increase in the specific area of the LSM electrode.

Keywords: Electrical conductivity; Fuel cells; Perovskites; Ionic conductivity; $LaGaO_3$

1. Introduction

The solid oxide fuel cells are under development for the generation of electricity with little environmental pollution. Since lowering the operating temperature has many advantages, such as the broad choice of cheap interconnect materials and the long-term stability of cell components, much effort have been concentrated on finding an electrolyte material with higher ionic conductivity than yttria stabilized zirconia (YSZ) that is commercially used as an electrolyte for SOFCs.[1–3]

An electrolyte for SOFCs is required not only to have high oxygen-ion conductivity but also to have a high stability under severe operating conditions, such as high temperature and large oxygen-partial pressure (P_{O_2}) gradients for a long time. Previous studies[4–7] showed the degradation of LSGM electrolyte during sintering at high temperature or operating in reducing atmosphere. LSGM easily decomposes, especially when sintered at temperature greater than 1600 °C, due to the tendency of gallium(III) oxide reduction to gallium(I) oxide.[4] Yamaji and co-workers[5–7] examined the chemical stability of LSGM in reducing atmosphere. They showed that the migration of Si and Al from Pyrex sealant and Pt from electrode into the surface of LSGM electrolyte is responsible for a depletion of Ga from LSGM electrolyte.[5] The reaction of Ga_2O_3 with H_2 in very low P_{O_2} resulted in the formation of Ga_2O and H_2O (vaporization of Ga).[6] Doping of lanthanum gallate with Sr and the presence of Pt enhanced the depletion of Ga from the electrolyte in the reducing atmosphere.[7]

Examination of P_{O_2} dependence of overpotential is one method to determine the reduction mechanism of LSGM. As P_{O_2} decreases, the cathodic overpotential increases with applied current. High cathodic overpotential tends to reduce the electrolyte. However, the effect of high potential on the cathode and electrolyte due to the applied current is not yet clear for LSGM electrolyte-based fuel cells. In this study, the change in cathode performance and electrolyte properties under high overpotential condition was examined.

2. Experimental

Stoichiometric amount of La_2O_3 (99.99%, Strem Chemicals, USA), $SrCO_3$ (99.9%, High Purity Chemicals, Japan), and Mn_2O_3 (99.9%, High Purity Chemicals) powders were

* Corresponding author. Tel.: +82 562 279 2146; fax: +82 562 279 2399.
E-mail address: gmchoi@postech.ac.kr (G.M. Choi).

0955-2219/$ – see front matter © 2005 Elsevier Ltd. All rights reserved.
doi:10.1016/j.jeurceramsoc.2005.03.118

mixed to prepare LSM ($La_{0.9}Sr_{0.1}MnO_3$) electrode, and La_2O_3, $SrCO_3$, Ga_2O_3 (99.9%, High Purity Chemicals) and MgO (99.9%, High Purity Chemicals) powders for LSGM electrolyte. The powder mixtures were ball-milled with zirconia balls in distilled water for 12 h, and calcined at 1200 °C for 6 h. The calcined LSGM powder was formed into disc-shape by die pressing, followed by cold isostatic pressing at 200 MPa and sintering at 1500 °C for 6 h in air with the heating/cooling rate of 3 °C/min. Sintered LSGM pellet (~97% relative density) was sliced into thin disks of ~500 μm.

The calcined LSM powders were screen-printed on LSGM electrolyte and heat treated or sintered at 1300 °C in air for 2 h. Three-electrode configuration cells were fabricated; the working electrode is a cathode under investigation and the counter and the reference electrodes are platinum at the opposite side of the working electrode. The cell was heated for 1 h at 1000 °C after Pt pasting (Engelhard No. 6926, USA). Pt mesh (Aldrich 52 mesh, USA), as a current collector, was bonded at 1000 °C for 1 h to the three electrodes.

The ohmic- and the over-potential values were measured by using a current interruption device (Doosung Induction, DSI-10, Korea), a current source (Solartron, SI 1287, UK) and digitizing oscilloscope (Tektronix, TDS 3032, USA). The electrochemical measurement was performed between 800 and 900 °C in P_{O_2} between 1 and 0.003 atm. The cathodic overpotential changed with time and reached its steady state value within 10 min at high P_{O_2}, and within 1 h at $P_{O_2} = 0.003$ atm. Microstructure was observed by a field-emission scanning electron microscope (JEOL, model 6330F, Japan).

3. Results and discussion

The cathodic overpotential of LSM electrode as a function of current density is shown in Fig. 1. The cathodic overpotential at 1 atm of P_{O_2} (1 atm (before)) increased slowly as the current density increased. The curves obtained at P_{O_2} greater than 0.015 atm showed the similar trend as the 1-atm curve. However, at $P_{O_2} = 0.003$ atm, the cathodic overpotential increased sharply with current density. Such an increase is often due to a diffusion limiting process. Oxygen cannot be supplied fast enough from cathode to electrolyte with increasing current density. The cathodic overpotential value at 100 mA/cm^2 of current density was ~1.85 V. Hereafter, we refer the measurement under 1.85 V at 800 °C, $P_{O_2} = 0.003$ atm as the low P_{O_2} measurement. The cathodic overpotential value was measured again at 1 atm after the low P_{O_2} measurement and it (1 atm (after)) was smaller than the initial value (1 atm (before)). The decrease in overpotential after the low P_{O_2} measurement needs explanation. Garbage et al.[8] reported that oxygen vacancies were created in the LSM electrode at high polarization, and the cathodic reaction was progressively delocalized over the whole surface of the electrode. During the low P_{O_2} measurement, the sample was maintained under high overpotential (~1.85 V) and thus

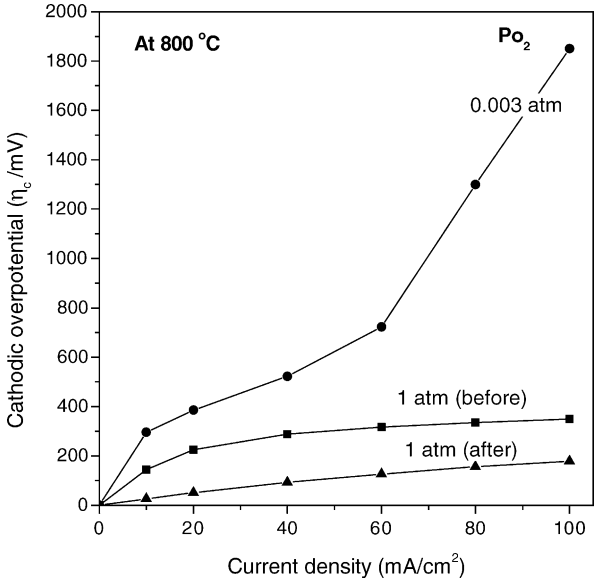

Fig. 1. The cathodic overpotential of Pt/LSM/LSGM/Pt cell measured at 800 °C as a function of current density in $P_{O_2} = 1$ and 0.003 atm. It was measured in a P_{O_2} of 1 atm (before), 0.003 atm and again 1 atm (after).

oxygen vacancies may have been created in LSM electrode. The P_{O_2} equilibrated with external electromotive force (emf) follows the Nernst equation:

$$\text{emf} = -\frac{RT}{4F}\ln\frac{P''_{O_2}}{P'_{O_2}} \quad (1)$$

where R, T, P'_{O_2} and P''_{O_2} are the gas constant, the absolute temperature, the reference P_{O_2}, and the equilibrated P_{O_2}. Since the reference P_{O_2} was 0.003 atm and the emf value was 1.85 V, the P''_{O_2} may be as low as 3.65×10^{-36} atm at 800 °C. Such a highly reducing P_{O_2} enhances the formation of oxygen vacancies in LSM electrode.

The effect of reduction potential on the cathode performance was examined. Fig. 2 shows the temperature dependence of polarization conductance (G_p) at 40 mA/cm^2 of current density. The polarization conductance was defined as:

$$\frac{1}{G_p} = R_p = \frac{\eta_c}{J} \quad (2)$$

where R_p is the polarization resistance, η_c is the cathodic overpotential and J is the current density.

The polarization conductance at 1 atm increased after the low P_{O_2} measurement at 0.003 atm. The activation energy (E_a) of G_p of LSM electrode at 1 atm is similar before and after the low P_{O_2} measurement (0.73 ~ 0.75 eV). The reported activation energy values of G_p are known to be varying depending on the combination of electrode and electrolyte. For YSZ electrolyte, $La_{0.7}Sr_{0.3}MnO_3$ and $La_{0.7}Sr_{0.3}CoO_3$ electrodes, E_a has a value of 1.87 and 2.28 eV,[9] respectively, and 1.49 eV[10] for $La_{0.8}Sr_{0.2}MnO_3$–YSZ composite electrodes. For $La_{0.6}Sr_{0.4}CoO_3$ and $La_{0.9}Sr_{0.1}Ga_{0.5}Ni_{0.5}O_3$ electrodes on LSGM electrolyte, E_a has a value of 0.96 and 1.816 eV.[11] Finally, for $La_{0.6}Sr_{0.4}Co_{0.98}Ni_{0.02}O_3$, $La_{0.6}Sr_{0.4}CoO_3$ and Pt

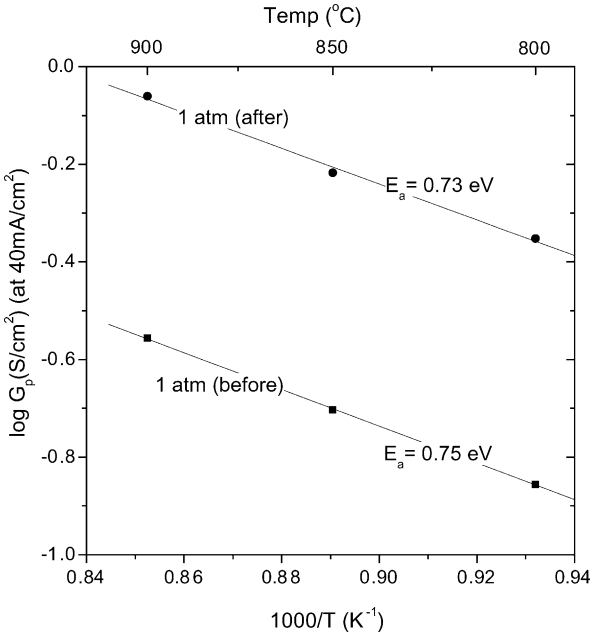

Fig. 2. Temperature dependence of polarization conductance of LSM cathode measured at 40 mA/cm^2 before and after the low P_{O_2} (0.003 atm) measurement.

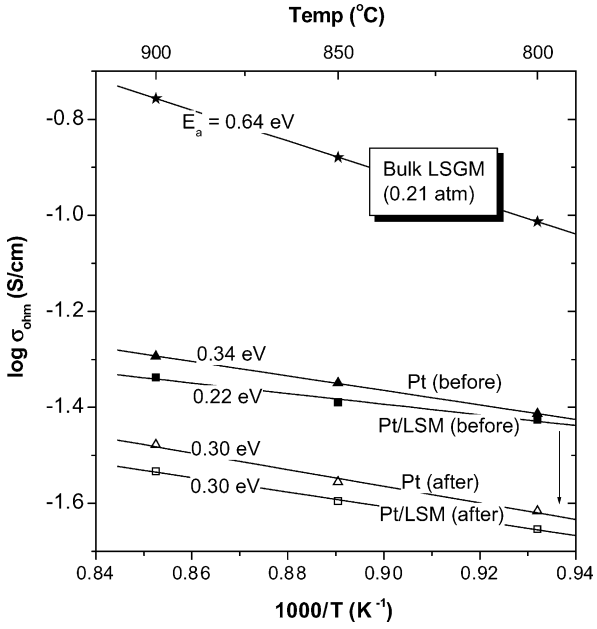

Fig. 4. Temperature dependence of the conductivity of LSGM electrolyte measured in oxygen atmosphere before and after the low P_{O_2} measurement. Pt/LSM, Pt in the figure indicate Pt/LSM/LSGM/Pt cell and Pt/LSGM/Pt cell, respectively. The evolution of the conductivity of LSGM electrolyte in 0.21 atm is given for comparison.

electrodes on $(CeO_2)_{0.9}(CaO)_{0.1}$ electrolyte, E_a was 0.5, 0.63 and 1.13 eV, respectively.[12] Generally, the electrodes having the charge transfer reaction as the rate-determining step of oxygen reduction have high activation energies of G_p. The observation of no change in E_a after the low P_{O_2} measurement tells us that no electrode composition or oxygen-reduction mechanism has been changed.

The microstructures of the LSM electrode (a) before and (b) after the low P_{O_2} measurement are shown in Fig. 3. After the low P_{O_2} measurement, more porous morphology was shown. The change in electrode morphology was irreversible and the porous morphology after the low P_{O_2} measurement did not convert to its original morphology in oxygen. Since the activation energy of G_p did not change before and after the low P_{O_2} measurement, the change in G_p was due to the microstructural change rather than the compositional change of electrode as discussed above. The creation of oxygen vacancies and thus the increase in the specific area of the electrode could be the reasons for the increase in the polarization conductance.

In order to see the effect of the low P_{O_2} measurement on the electrolyte, the conductivity of the electrolyte was examined. Fig. 4 shows the temperature dependence of the ohmic conductivity (σ_{ohm}). The ohmic conductivity is defined as:

$$\sigma_{ohm} = \frac{1}{R_{ohm}} \times \frac{t}{A} \quad (3)$$

where R_{ohm} is the ohmic resistance of cell determined from current-interruption measurement, t is the electrolyte thickness, and A is the electrode area. Fig. 4 also includes conductivity measurements by using four-probe dc method on the LSGM electrolyte alone.[13] Both open and closed square symbols represent the conductivity of LSGM measured from the

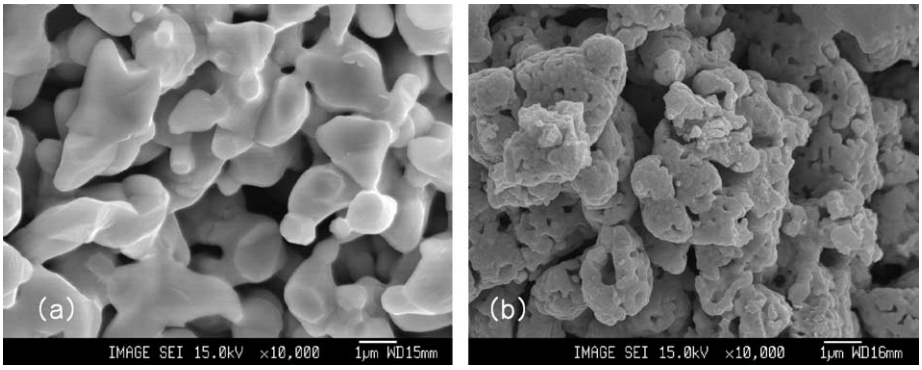

Fig. 3. SEM pictures of LSM electrode (a) before and (b) after the low P_{O_2} (0.003 atm) measurement.

current-interruption method that deconvolutes ohmic-voltage drop from non-ohmic overpotential. Both the values and the activation energy of the conductivity were smaller than those of bulk LSGM. The smaller value of ohmic conductivity of the cell may partly be due to the reaction layer formed between LSM electrode and LSGM electrolyte during the cell preparation.[14] The reaction product should show much lower conductivity than either LSM or LSGM. The reaction layer is also responsible for the reduced activation energy in comparison with that of the bulk LSGM.[13] In other words, the contribution of the reaction layer to the ohmic resistance is large enough to change the measured conductivity of LSGM electrolyte. After the low P_{O_2} measurement, further decrease in ohmic conductivity was observed as shown by open square symbols in Fig. 4. At first, we thought the decrease was due to the additional reaction between LSM electrode and LSGM electrolyte. To verify the reason for the further decrease in ohmic conductivity after the low P_{O_2} measurement, we fabricated and tested the Pt/LSGM/Pt cell (without LSM electrode). Although the Pt/LSGM/Pt cell does not have LSM electrode, the decrease in ohmic conductivity after the low P_{O_2} measurement was also observed (open and solid triangle symbols in Fig. 4). Thus, we think that the additional decrease after the low P_{O_2} measurement is not due to the further reaction between LSM and LSGM but due to the change in LSGM composition during electrochemical measurement.

We have also examined the dependence of the ohmic conductivity of the cell with the P_{O_2}. The ohmic conductivity was nearly constant in all P_{O_2} above 0.01 atm. If the migration of B-site ions continues during electrochemical measurement, the ohmic conductivity may vary with P_{O_2}. This is a proof that there is no further reaction between LSM and LSGM during 800 ∼ 900 °C measurement. The change in ohmic conductivity of LSGM only occurs after the low P_{O_2} measurement.

The microstructures of the cell (Pt/LSM/LSGM/Pt) after the low P_{O_2} measurement are shown in Fig. 5. The LSGM electrolyte near LSM cathode became porous and small grains are visible on Fig. 5a. In contrast, the original LSGM electrolyte (far right side of Fig. 5b) is dense. This porous area was formed due to the decomposition of LSGM electrolyte. Approximately 100 μm away from LSM electrode, needle-shaped phases were newly formed. We named this area as a decomposition front in Fig. 5b. The decomposition front moves away from the LSM/LSGM interface to the counter electrode (Pt) with time during the low P_{O_2} measurement. We also characterized cells using either 0.4LSM-0.6LSGM composite (Pt/0.4LSM-0.6LSGM/LSGM/Pt) or Pt (Pt/LSGM/Pt) as a cathode, the same decomposition behavior (i.e. porous decomposition layer and needle-shaped phase in decomposition front) was observed. In all cells, decomposition of the LSGM electrolyte initiates near cathode/electrolyte interface. The decomposition front was found at around 80 μm from the Pt cathode for the Pt/LSGM/Pt cell. For this cell, the overpotential due to the applied current of 100 mA/cm^2 was 1.65 V. The closer location (∼80 μm) of the decomposition front from cathode for the Pt cathode than that (∼100 μm) for the LSM cathode is reasonable considering the smaller potential for the Pt cathode (1.65 V) than the LSM cathode (1.85 V). As the overpotential increases, the reduction of cathode side become more severe and a wider decomposition layer is expected at the electrolyte/cathode interface.

During the low P_{O_2} measurement, the overpotential may be concentrated on the cathode/electrolyte interface due to the higher overpotential than the ohmic potential. A reducing atmosphere as low as 3.65×10^{-36} atm can be developed at the interface for Pt/LSM/LSGM/Pt cell. This reduction potential is possible if the oxygen flow is partially blocked. The reported decomposition P_{O_2} for LSGM at 800 °C is $\sim 10^{-22}$ atm.[5,15] Thus, we need only ∼1.04 V to obtain $\sim 10^{-22}$ atm with respect to the counter electrode potential. Although the actual P_{O_2} at the decomposition front is not clear due to the unknown potential distribution across the cell, the P_{O_2} at the decomposition front may be as low as 10^{-22} atm when the cathode works as a current limiting or an ion-blocking electrode.

To determine the phases formed in the decomposition layer, the Pt/LSGM/Pt cell was maintained at low P_{O_2} (0.003 atm) at 800 °C, while supplying 100 mA/cm^2 (∼1.65 V of overpotential) for ∼10 h. The resultant cell was crushed and examined by X-ray diffraction. In addition to the original LSGM phase, La_2O_3, $La(OH)_3$ and $LaSrGaO_4$ were observed. The white powders observed on the Pt cathode surface was identified as La_2O_3 and $La(OH)_3$. These phases probably formed as a result of Ga evapora-

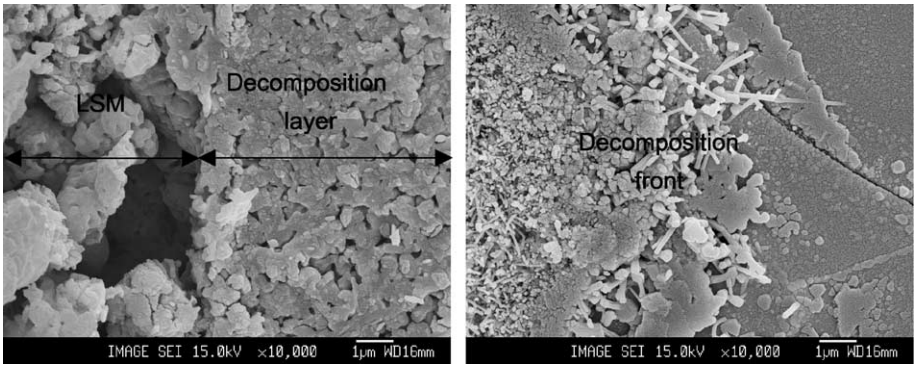

Fig. 5. SEM pictures of (a) decomposition layer and (b) decomposition front of Pt/LSM/LSGM/Pt cell after the low P_{O_2} measurement.

tion on the cathode surface that was exposed to the reducing atmosphere.[6,7] $LaSrGaO_4$ is a Sr-rich $LaGaO_3$ phase. No Mg-excess phase was observed. Mg is probably contained in La_2O_3 or $LaSrGaO_4$ as a solid-solution component.[6]

4. Conclusions

The cathodic overpotential of LSM/LSGM/Pt cell at low P_{O_2} (0.003 atm) increased sharply as the current density increased due possibly to the limited oxygen diffusion at the cathode. As a result of reduction, the polarization conductance increased due to the formation of a porous LSM cathode. The conductivity of the LSGM electrolyte decreased since the LSGM electrolyte decomposed in reducing atmosphere. The decomposition layer formed near the cathode was porous and had small grains. Needle-shaped phases were formed at the decomposition front. The main decomposition phases of the LSGM electrolyte are La_2O_3, $La(OH)_3$ and $LaSrGaO_4$.

Acknowledgements

This work was supported by the BK 21 Project. The authors thank to Doosung Induction Co. for the support of the electronic switch that enables the current interruption measurement.

References

1. Minh, N. Q., *J. Am. Ceram. Soc.*, 1993, **76**, 563.
2. Ishihara, T., Matsuda, H. and Takita, Y., *J. Am. Chem. Soc.*, 1994, **116**, 3801.
3. Wachsman, E. D., Jayaweera, P., Jiang, N., Lowe, D. M. and Pound, B. G., *J. Electrochem. Soc.*, 1997, **144**, 233.
4. Stevenson, J. W., Armstrong, T. R., Pederson, L. R., Li, J., Lewinsohn, C. A. and Baskaran, S., *Solid State Ionics*, 1998, **113–115**, 571.
5. Yamaji, K., Horita, T., Ishikawa, M., Sakai, N. and Yokokawa, H., *Solid State Ionics*, 1998, **108**, 415.
6. Yamaji, K., Horita, T., Ishikawa, M., Sakai, N. and Yokokawa, H., *Solid State Ionics*, 1999, **121**, 217.
7. Yamaji, K., Negishi, H., Horita, T., Sakai, N. and Yokokawa, H., *Solid State Ionics.*, 2000, **135**, 389.
8. Garbage, B., Pannier, T. and Hammer, A., *Electrochim. Act.*, 1994, **141**, 2118.
9. Takeda, Y., Kino, R., Noda, M., Tumid, Y. and Yamamoto, O., *J. Electrochem. Soc.*, 1987, **134**, 2656.
10. Murray, E. P., Tsai, T. and Barnett, S. A., *Solid State Ionics*, 1998, **110**, 235.
11. Lecarpentier, F., Tuller, H. L. and Long, N., *J. Electroceram.*, 2000, **5**, 225.
12. Inoue, T., Seki, N., Eguchi, K. and Arai, H., *J. Electrochem. Soc.*, 1990, **137**, 2523.
13. Yi, J. Y. and Choi, G. M., *Solid State Ionics*, 2002, **148**, 557.
14. Yi, J. Y. and Choi, G. M., *J. Eur. Ceram. Soc.*, 2004, **24**, 1359.
15. Huang, K., Feng, M., Goodenough, J. B. and Schmerling, M., *J. Electrochem. Soc.*, 1996, **143**, 3630.